Semiclassical Approach for Bifurcations in a Smooth Finite-Depth Potential

Alexander G. Magner,[1,3,4,5] Ken-ichiro Arita[2] and Sergey N. Fedotkin[4,5]

[1]*Department of Physics, Graduate School of Science, Kyoto University, Kyoto 606-8502, Japan*
[2]*Department of Physics, Nagoya Institute of Technology, Nagoya 466-8555, Japan*
[3]*Laboratoire de Spectrométrie Physique, Université Joseph-Fourier-Grenoble, F-38402 Saint-Martin-d'Hères Cedex, France*
[4]*Institute for Nuclear Research, 03680, Prospekt Nauki 47, Kiev-28, Ukraine*
[5]*Institute for Theoretical Physics, University of Regensburg, D-93040 Regensburg, Germany*

The analytical trace formula for a dense cascade of bifurcations was derived using the improved stationary phase method based on extensions of the semiclassical Gutzwiller path integral approach. For the integrable version of the famous Hénon-Heiles Hamiltonian, our analytical trace formula solves all bifurcation problems, in particular, in the harmonic oscillator limit and the potential barrier limit. We obtain nice agreement with quantum results for gross to finer shell structures in level densities and for the shell structure energies, even near the potential barrier where there is a rather dense sequence of bifurcations.

§1. Introduction

The Gutzwiller trace formula[1),2)] and its extensions to continuous symmetries[3)–9)] are nice tools to study shell structures in finite fermionic systems. This is the so-called periodic orbit theory (POT), which relates quantum fluctuations in single-particle level densities to classical periodic orbits through their dynamical characteristics, such as action integrals, stability matrices, and degeneracy (symmetry) parameters.

Recently, the POT was employed in studies seeking to overcome some symmetry-breaking problems related to divergencies and discontinuities of the standard stationary phase method (standard SPM, SSPM)[2),9)] due to a bifurcation phenomenon. For instance, the improved stationary phase method (ISPM) within the extended Gutzwiller approach (EGA)[10)–12)] was used in derivations of the trace formulas. The ISPM is based on the theory of critical caustics and turning points formulated by Maslov and Fedoryuk[13)–17)] in order to overcome bifurcation problems. Furthermore, the idea of Berry and Tabor[5)] has been applied to calculate catastrophe integrals more exactly within finite limits over the accessible phase space volume for classical motion.

Other semiclassical approaches, known as the uniform approximations, were suggested and successfully developed previously[18)–26)] on the basis of the theory of

normal forms[27),28)] and perturbation theory.[9),29)] In practical applications of some analytical normal forms to generating functions, local expansions near the bifurcation point and the consistency with the known asymptotic SSPM trace formulas far from bifurcations were used in solving the bifurcation problems in the description of the coarse-grained gross shell structures of averaged level densities.[9),20),26)]

For many Hamiltonians with barriers, like the famous Hénon-Heiles (HH) and its integrable (separating) version (IHH),[9),26),30)–32)] one encounters a very dense cascade of bifurcations, infinitely dense at the barrier. In the POT calculations of Strutinsky[33)] the shell-structure energy and the coarse-grained level density with smaller averaging parameter, bifurcations appear rather frequently. In such cases, the SSPM fails in the entire region between adjacent bifurcation points, and therefore it might be inconvenient to use the known asymptotic solutions of the SSPM for matching with the local expansions mentioned above at each bifurcation, especially near the barrier. We may also expect a sharp enhancement in the density amplitudes of order of $\hbar^{-1/2}$ for increasing classical degeneracy by one unit, as formulated in the ISPM for several Hamiltonians, near the bifurcations due to a local symmetry breaking.[10)–12)] In order to solve such bifurcation problems, alternative methods, like ISPM,[10)–12)] which does not use smooth interpolations through the bifurcations in terms of the normal forms and the asymptotic SSPM trace formulas, might be helpful, for instance, for comparison with the uniform approximations and understanding the relation to the EBK formulation.[26)]

In the present paper, we apply the ISPM[10)–12)] to the general case of a dense bifurcation cascade, employing the IHH Hamiltonian as a simple, analytically solvable, and non-trivial example. The classical dynamics and bifurcations of the periodic orbits are considered in §2. The ISPM trace formula for this Hamiltonian is derived in §3. Then, in §4 we compare our semiclassical densities and shell structure energies with the quantum mechanical ones. Section 5 summarizes the results.

§2. Periodic orbits and their bifurcations

The IHH Hamiltonian is expressed in Cartesian coordinates as[9),26)]

$$H = \frac{1}{2}\left(p_x^2 + p_y^2\right) + \frac{1}{2}\left(x^2 + y^2\right) - \frac{\epsilon}{3}\,y^3. \tag{1}$$

It can be decomposed into x and y components, and we define energies corresponding to motion along each of these directions: $E = E_x + E_y$ with $E_x = (p_x^2 + x^2)/2$, $E_y = (p_y^2 + y^2)/2 - \epsilon\, y^3/3$. Then, making use of the scaled variables ϵx and ϵy, we can see that the classical dynamics are controlled by the single energy parameter E/E_b, where $E_b = 1/6\epsilon^2$ is the barrier energy.[9),26)] Nevertheless, we explicitly keep ϵ in the following derivations to study the ϵ dependence of the trace formulas.

In action-angle variables, this Hamiltonian $H = H(\boldsymbol{I})$ is a function of only the action variables $\boldsymbol{I} = \{I_x, I_y\}$:[26)]

$$I_x = \frac{1}{2\pi}\oint dx\, p_x = E_x = E - E_y,$$

$$I_y = \frac{1}{2\pi} \oint dy\, p_y = \frac{12a}{10\pi\epsilon^2}\, [\mathrm{E}(q) + c\mathrm{K}(q)]. \tag{2}$$

Here, $\mathrm{K}(q)$ and $\mathrm{E}(q)$ are complete elliptic integrals of the first and second kinds, we have $c = -(2/9)\,\epsilon^2(y_3-y_2)(2y_3-y_2-y_1), a = \sqrt{\epsilon(y_3 - y_1)/6}, q = \sqrt{(y_2 - y_1)/(y_3 - y_1)}$, the quantities $y_n = \{1/2 - \cos[(\phi + \pi(2n - 3))/3]\}/\epsilon$ $(n = 1, 2, 3)$ are the turning points at a given energy E_y, and $\phi = \arccos(1 - 12E_y\epsilon^2)$. The equations of classical motion with the Hamiltonian (1) are easily integrated, yielding

$$x(t) = \sqrt{2I_x}\, \sin\left(t + \Theta'_x\right), \qquad y(t) = y_1 + (y_2 - y_1)\,\mathrm{sn}^2(at + \Theta'_y, q), \tag{3}$$

where Θ'_x and Θ'_y are integral constants determined by the initial conditions, and $\mathrm{sn}(z, q)$ is the Jacobi elliptic function.

A canonical transformation from the Cartesian variables $\{\boldsymbol{r}, \boldsymbol{p}\}$ to the action-angle variables $\{\boldsymbol{\Theta}, \boldsymbol{I}\}$ can be obtained explicitly. For the x components, we have the harmonic oscillator (HO) relations,

$$x = \sqrt{2I_x}\, \sin\Theta_x, \qquad p_x = \sqrt{2\,I_x}\, \cos\Theta_x. \tag{4}$$

Because the angles Θ_i $(i = x, y)$ are cyclic variables in the integrable Hamiltonian (1), the classical trajectories can be written in the usual way,

$$\Theta_i = \omega_i\, t + \Theta'_i, \qquad I_i = \mathrm{const},$$

where the quantities $\omega_i = \partial H/\partial I_i$ are the frequencies

$$\omega_x = 1, \qquad \omega_y = \frac{\pi a}{\mathrm{K}(q)}.$$

The periodic orbit equation can be written as a relation expressing the commensurability of the frequencies ω_i (a resonance condition):

$$\frac{\omega_x}{\omega_y} \equiv \frac{\mathrm{K}(q)}{\pi a} = \frac{n_x}{n_y}. \qquad (n_x \geq n_y > 0) \tag{5}$$

Here, n_x and n_y are relatively prime integers which specify the primitive periodic orbits. We denote the periodic orbits β through these integers $\beta = M(n_x, n_y)$, where M is the number of repetitions.

There are two kinds of periodic orbits in the IHH potential, one-parameter *families* with the degeneracy parameter $\mathcal{K} = 1$, and *isolated* periodic orbits $(\mathcal{K} = 0)$.[*] Some examples of the simplest periodic orbits are displayed in Fig. 1. Figure 2 displays important characteristics of such periodic orbits, the periods $T_y = 2\mathrm{K}(q)/a$

---

[*] The degeneracy (symmetry) parameter $\mathcal{K}$ is defined by the number of independent parameters of the periodic orbit with the same action at a given energy E in the phase space.[4] This $\mathcal{K}$ is equal to the number of independent single-valued integrals of motion, excluding the energy E. For integrable systems, one can integrate the resonance condition $\omega_i/\omega_j = n_i/n_j$ $(\omega_i = \partial H/\partial I_i = \dot{\Theta}_i,$ $i, j = 1, 2, \cdots, n$ for n degrees of freedom), resulting in the integral of motion $\Theta_i n_j - \Theta_j n_i = \mathrm{const}$. Its periodic function, for example $\sin(\Theta_i n_j - \Theta_j n_i)$, is a single-valued integral of motion other than the energy.[7]
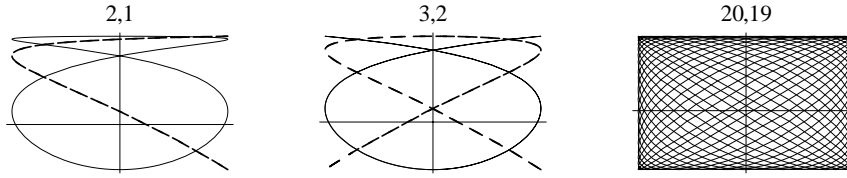
Fig. 1.   Examples of the periodic orbits (n_x, n_y) (solid and dash ed) in the IHH potential.
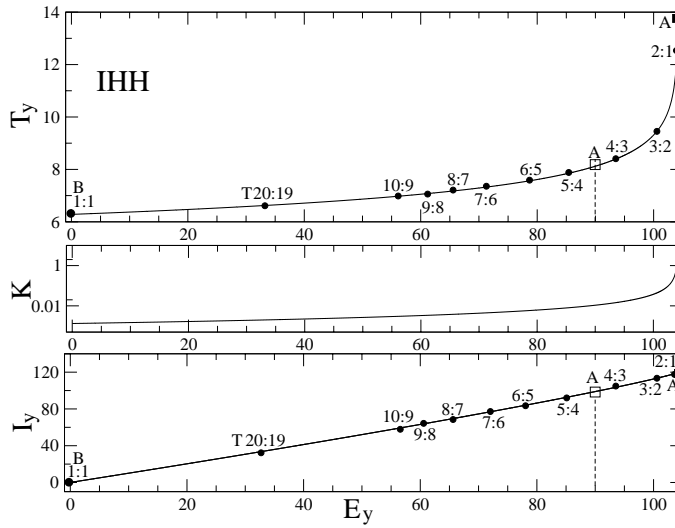

Fig. 2.   The period T_y (top), the energy surface $I_y = I_y(E_y)$ (bottom), and its curvature K (middle). The dots represent the bifurcations for some families T and B. The filled square is related to the isolated orbit A at the barrier energy $E = E_b \approx 104$, and the unfilled square corresponds to the isolated orbit A at the energy $E = 90$. Here, we use $\epsilon = 0.04$ as an example.

in the top panel, the energy curve $I_y = I_y(E_y)$ in the bottom, and its curvature $K = \partial^2 I_y / \partial E_y^2$ in the middle. The expressions $n_x : n_y$ indicate the bifurcations of the periodic orbits which form *families.*

In addition to the two-dimensional orbits T $(n_x > n_y)$, such as those shown in Fig. 1, there are two straight linear orbits along x and y axes. The orbits B along the x axis, described by the first equation of (3) and shown in Fig. 2 at $n_x : n_y = 1 : 1$, form specific *local* one-parameter $(\mathcal{K} = 1)$ families. They are similar to the repeated short diameters (SD) in elliptic billiard systems at the bifurcation deformations.[10] It should be noted that the orbits B form local families for any value of ϵ, because the term ϵy^3 represents a higher-order perturbation for orbits B $(y = 0)$ and does not affect their local properties. This fact can be confirmed by direct calculations of the trace of the stability matrix Tr M for the orbit B, which leads to Tr $M = 2$, independently of ϵ.[34] The resonance equation (5) specifies one of the constants of motion, for instance I_x in (3) through its solution $E_y = 0$ for B orbits ($E_y > 0$ for T orbits). However, due to the relation in (5), another single-valued integral of motion, $\sin(\Theta'_y n_x - \Theta'_x n_y)$, appears for $n_x = n_y = 1$ ($n_x > n_y$ for T orbits) at a given energy E [see the footnote referred to after Eq. (5)]. For B orbits, for instance, the

initial value Θ'_x can be set to zero without any restriction, and $\sin(\Theta'_y)$ can be *locally* considered a single-valued parameter of the family of orbits B, like SD [$\sin(\Theta'_u)$ in elliptic u, v coordinates[10]] at the bifurcation deformations in elliptic billiards. (See Refs. 4), 7) and 35) for studies of general integrable systems.) In the following, we refer to such specific local families simply as 'families'.

Other linear orbits along the y axis are the isolated orbits A given by the second equation in (3). One such orbit is denoted by the unfilled square at the endpoint $E_y = E$ of the interval $0 \le E_y \le E$ in Fig. 2. The orbit A crosses the bifurcation points (indicated by dots) at the energy $E = E_{\mathrm{bif}}$ with increasing energy E. New families are born at these points and coexist with A for larger energies E up to the barrier energy E_b. Note that the orbits A form local one-parameter families at the bifurcation points for the same reasons as in the case of the SD in elliptic billiard.

§3.   ISPM trace formulas

3.1.   *Phase space trace formulas*

The level density $g(E)$ for the 2-dimensional Hamiltonian $H(\boldsymbol{r}, \boldsymbol{p})$ in Cartesian coordinates and momenta $\{\boldsymbol{r}, \boldsymbol{p}\}$ can be obtained within the EGA from the phase-space trace formula:[10), 21), 36)]

$$g(E) = \sum_i \delta\left(E - E_i\right)$$

$$\simeq \mathrm{Re} \sum_\alpha \int \frac{d\boldsymbol{r}' d\boldsymbol{p}''}{(2\pi\hbar)^2} \delta\left(E - H(\boldsymbol{r}'', \boldsymbol{p}'')\right) |\mathcal{J}_\alpha|^{1/2} \exp\left[\frac{i}{\hbar}\Phi_\alpha - i\frac{\pi}{2}\mu_\alpha\right]$$

$$= \mathrm{Re} \sum_\alpha \int \frac{dx' dp''_x}{(2\pi\hbar)^2} T_{y\,\alpha} |\mathcal{J}_\alpha|^{1/2} \exp\left[\frac{i}{\hbar}\Phi_\alpha - i\frac{\pi}{2}\mu_\alpha\right]. \quad (6)$$

In the first line here, E_i represents the quantum energy level. In the last two lines, the summation is taken over all (both closed and unclosed) classical trajectories α for particle motion that starts with the initial coordinate $\boldsymbol{r}'$ and ends with the final momentum $\boldsymbol{p}''$ at a given energy E. The quantity μ_α is the Maslov phase determined by the number of *conjugate* (turning and caustics) points[13)–16)] along α, $T_{y\,\alpha}$ is the period of motion along the y direction, and $\mathcal{J}_\alpha$ is the Jacobian $\mathcal{J}_\alpha(p'_x, p''_x)$ for transformations from the initial momentum component, p'_x, to the final one, p''_x, perpendicular to the periodic orbit β (see below).

For given $\boldsymbol{r}'$, $\boldsymbol{p}''$ and energy E, there exists a unique trajectory α, regardless of the existence of continuous symmetries. The integrations in the third line are carried out only over the phase-space variable components x' and p''_x, perpendicular to the periodic orbit β. The latter is specified below in a local coordinate system consisting of $\boldsymbol{r} = \{x, y\}$ and $\boldsymbol{p} = \{p_x, p_y\}$, where y and p_y are directed along β, as in Refs. 1), 2), 4) and 9). The phase Φ_α in Eq. (6) is given by the Legendre transformation as

$$\Phi_\alpha(\boldsymbol{r}', \boldsymbol{p}'', E) \equiv S_\alpha(\boldsymbol{p}', \boldsymbol{p}'', t_\alpha) + (\boldsymbol{p}'' - \boldsymbol{p}') \cdot \boldsymbol{r}' = S_\alpha(\boldsymbol{r}', \boldsymbol{r}'', E) - \boldsymbol{p}'' \cdot (\boldsymbol{r}'' - \boldsymbol{r}'), \quad (7)$$

which relates the action $S_\alpha(\boldsymbol{p}', \boldsymbol{p}'', t_\alpha)$ in the momentum representation to the action

$S_\alpha(\boldsymbol{r}', \boldsymbol{r}'', E)$ in coordinate space:

$$S_\alpha(\boldsymbol{p}', \boldsymbol{p}'', t_\alpha) = - \int_{\boldsymbol{p}'}^{\boldsymbol{p}''} d\boldsymbol{p} \cdot \boldsymbol{r}(\boldsymbol{p}), \qquad S_\alpha(\boldsymbol{r}', \boldsymbol{r}'', E) = \int_{\boldsymbol{r}'}^{\boldsymbol{r}''} d\boldsymbol{r} \cdot \boldsymbol{p}(\boldsymbol{r}). \qquad (8)$$

For calculation of the trace integral using the SPM, first we have to write the *stationary phase* conditions in the perpendicular variables x' and p_x'':

$$\left(\frac{\partial \Phi_\alpha}{\partial p_x''}\right)^* \equiv \left(x' - x''\right)^* = 0, \qquad \left(\frac{\partial \Phi_\alpha}{\partial x'}\right)^* \equiv -\left(p_x' - p_x''\right)^* = 0. \qquad (9)$$

We use the asterisk both here and below to indicate that the quantity is taken at the stationary point. We used the first and second equations in Eq. (7) for the derivations of these SPM conditions with respect to p_x'' and x', respectively.[2),9)] Because the variations of Φ_α are independent of the parallel coordinates, due to the energy conservation expressed explicitly in the second line of Eq. (6) through the δ function, there are two additional identities for the stationary-phase conditions in the parallel phase-space components y' and p_y''. These are written as $y' = y''$ and $p_y'' = p_y'$. With the stationary phase conditions (9), they are altogether identical to the *periodic orbit* equations. In the case of an integrable system, they are equivalent to the resonance relationships (5) for the partial frequencies.

For non-integrable Hamiltonians, we may find only isolated manifolds of stationary points related to the isolated periodic orbits. The integrable case is more rich in the sense that there also exist manifolds of the stationary points that form continuous families of the periodic orbits, along with the isolated ones.

Now, we describe the reason for the divergences in the isolated-orbit contributions and the discontinuities in the family-orbit contributions at the bifurcation potential parameter in SSPM. They are related to the *second-order* expansion of the phase Φ_α (7) near the stationary-phase bifurcation point defined by Eq. (A·2) in the catastrophe integrals, like Eq. (A·1), and, at the same time, with an extension of the limits of integration within the finite region of the classically accessible phase space to *infinities*. Taking these two assumptions together will fail because the bifurcation point can be considered the specific stationary-phase point, (A·2), which lies at the boundary of classically accessible region.

In order to solve this problem, we have found that the bifurcation point is similar to the *caustic* singularity considered by Fedoryuk within the catastrophe theory.[13)–16)] (With regard to a proof of the theorem concerning the Maslov index, see Appendix A.) As shown in Appendix A, we can truncate the action phase Φ_α at second order while taking into account the Maslov index if the third-order derivative of Φ_α at the stationary point is not zero, as in the derivation of the Maslov theorem. The catastrophe point with an infinite second derivative but a finite third derivative of the action phase Φ_α (which is a separatrix, like the turning point described in Appendix A) was considered in Refs. 10) and 12). However, in addition to Fedoryuk's catastrophe theory, we have to maintain physically accessible *finite* limits, because the caustic-like bifurcation point (A·2) belongs to the boundary of classical motion, as mentioned above.

For the case of integrable systems, it is helpful to transform the integration variables from Cartesian to action-angle variables, $\{\boldsymbol{\Theta}, \boldsymbol{I}\}$, in the phase-space trace formula (6):[10]

$$g_{\text{scl}}(E) = \frac{1}{(2\pi\hbar)^2} \,\text{Re} \sum_\alpha \int d\Theta'_x \int dI_x \, T_{y\,\alpha} \, \left|\mathcal{J}_\alpha(p''_x, p'_x)\right|^{1/2} \exp\left[\frac{i}{\hbar}\,\Phi_\alpha - \frac{i\pi}{2}\mu_\alpha\right].$$

(10)

Here, $\boldsymbol{I} = \{I_x, I_y\}$ and $\boldsymbol{\Theta}' = \{\Theta'_x, \Theta'_y\}$ are action-angle variables, I_x and Θ'_x are the components that are "perpendicular" in the sense that they are related to the local Cartesian coordinate x, perpendicular to the periodic trajectory β.[2] The stationary phase conditions for these "perpendicular" action-angle variables I_x and Θ'_x, together with two identities for the "parallel" ones, I_y and Θ'_y, related to the parallel coordinate y, determine the corresponding periodic orbit equations mentioned above in terms of new variables.

Thus, the problem we face in attempting to carry out further derivations of the POT trace formulas for the IHH potential is to find all kinds of stationary points, i.e., the families and isolated periodic orbits described in §2. Then, in order to solve the bifurcation problems, we calculate the phase space trace integrals using the ISPM, as mentioned above.

3.2. *Leading family* ($\mathcal{K} = 1$) *contribution*

The one-parameter ($\mathcal{K} = 1$) families of periodic orbits T and B in the IHH Hamiltonian form continuous manifolds of stationary points $\Theta'_x = \Theta^*_x$, where $0 \leq \Theta^*_x \leq 2\pi$, for the phase Φ_α in the trace integral in Eq. (10) within the phase space volume of the tori. Thus, the "perpendicular" Θ'_x-component of the stationary phase conditions for family contributions is the identity, and hence Θ^*_x can be considered a parameter of the periodic orbit family having the same action. The integration over Θ'_x in Eq. (10) gives a factor of 2π, and therefore, using $\mathcal{J}_\alpha(p''_x, p'_x) = 1$ for the contribution of the families into the level density (10), one finally arrives at

$$\delta g_{\text{scl}}(E) = \frac{2}{\hbar^2} \,\text{Re} \sum_{k_x, k_y} \int dE_y \, \frac{1}{|\omega_y|} \exp\left[\frac{2\pi i}{\hbar}\,(k_y I_y(E_y) + k_x(E - E_y)) - \frac{i\pi}{2}\mu_{k_x k_y}\right],$$

(11)

where $k_x = Mn_x, k_y = Mn_y, n_x \geq n_y \geq 1, M = 1, 2, \cdots$.[*] Due to time-reversal symmetry, we have taken the summation in Eq. (11) over only positive M and multiplied by an additional factor of 2.

Integrating over E_y in Eq. (11) with the ISPM,[10] we first expand the action phase Φ_α (7) in the exponent of Eq. (11) near the stationary point E^*_y to second order:

$$\Phi_\alpha \equiv 2\pi\left[k_y I_y(E_y) + k_x(E - E_y)\right] = S_\beta(E) + \pi M n_y K_\beta(E_y - E^*_y)^2. \quad (12)$$

---

[*] The difference between Eq. (11) and a similar trace formula obtained in Ref. 26) from the EBK quantization rules is that the latter has a wider integer summation range. Specifically, the range in Eq. (C15) of Ref. 26) includes all integer pairs k_x, k_y except for $(k_x, k_y) = (0, 0)$. (In Ref. 26), these are denoted by k_u and k_v.) For a more detailed explanations of the EBK method, see Refs. 5) and 9).

Here, S_β and K_β are the action and the energy surface curvature, respectively, for the periodic orbit β of one of the isolated families determined by Eq. (5),

$$S_\beta(E) = 2\pi M \left[n_y I_y(E_y^*) + n_x(E - E_y^*) \right], \qquad K_\beta = \left(\frac{\partial^2 I_y}{\partial I_x^2} \right)^* = \left(\frac{\partial^2 I_y}{\partial E_y^2} \right)^*. \quad (13)$$

Here M is the number of repetitions along the periodic orbit $\beta = M(n_x, n_y)$ and $I_y(E_y)$ is the energy surface [see (2) and Fig. 2]. We now substitute the expansion (12) into Eq. (11) and set the smooth pre-exponent factors to their values at the stationary point $E_y = E_y^*$. Then, taking the transformation of the variable E_y to the dimensionless variable z, given by $z = \sqrt{-i\pi M n_y K_\beta/\hbar} \left(E_y - E_y^* \right)$, we obtain the following contributions of the T and B ($\mathcal{K} = 1$) families:

$$\delta g_{\mathrm{scl}}^{(1)}(E) = \mathrm{Re} \sum_\beta \frac{T_\beta}{2\pi \sqrt{-iM n_y^3 \hbar^3 K_\beta}} \, \mathrm{erf}\left(\mathcal{Z}_\beta^+, \mathcal{Z}_\beta^- \right) \exp\left[\frac{i}{\hbar} S_\beta(E) - \frac{i\pi}{2} \mu_\beta \right]. \quad (14)$$

Here, the sum is taken over all discrete families T and B of the periodic orbits β. The families T emerge through bifurcations of the isolated orbit A at the energies E_{bif}, given implicitly by Eq. (5), and exist for all higher ones E up to the barrier value E_b. The family B is a specific family whose members are born exactly at the harmonic oscillator symmetry-breaking point $E_{\mathrm{bif}}=0$, as explained above. Their periods T_β are independent of the energy E, and are given by $T_\beta = 2\pi n_y/\omega_y = 2\pi n_x$ ($\omega_x = 1$). The stationary point E_y^* is equal to the bifurcation energy E_{bif} (see Fig. 2). The complex arguments $\mathcal{Z}_\beta^-$ and $\mathcal{Z}_\beta^+$ in the error function, $\mathrm{erf}(v, u) = 2 \int_u^v dz \, e^{-z^2}/\sqrt{\pi}$, are the limits of integration for the new variable z. They are expressed in terms of the curvature K_β (see Eq. (13)) at $E_y = E_y^*$ as

$$\mathcal{Z}_\beta^- = -\sqrt{-\frac{i\pi M n_y K_\beta}{\hbar}} \, b_\beta^{(1)} \left(E - E_y^* \right), \qquad \mathcal{Z}_\beta^+ = \sqrt{-\frac{i\pi M n_y K_\beta}{\hbar}} \, b_\beta^{(1)} E_y^*. \quad (15)$$

The coefficient $b_\beta^{(1)}$ is given approximately by $b_\beta^{(1)} = 1$ for families T ($n_x > n_y, M = 1, 2, \cdots$), and

$$b_\beta^{(1)} = 1 - \frac{1}{2} \exp\left[-\left(\frac{E}{2\Delta_{\mathrm{B}}} \right)^2 \right], \qquad \Delta_{\mathrm{B}} = \frac{1}{\sqrt{\pi M n_y K_{\mathrm{B}}/\hbar}} \quad (16)$$

for the orbits B ($n_x = n_y = 1$). In the HO limit ($E \to 0$), orbits A and B belong to the same $\mathcal{K} = 2$ family of the isotropic two-dimensional harmonic oscillator. In order for the contribution of these two families to occupy the same size of the manifold in this limit, we change the upper limit of the ISPM integration over E_y in Eq. (11) sharply from E to $E/2$ within a small energy dispersion $2\Delta_{\mathrm{B}}$ in the limit $E \to 0$. The transition width Δ_{B} is determined from the Gaussian-like form of the exponent with the phase Φ_α given by Eq. (12). (A more detailed explanation is given in Appendix B.) The remaining part of the integration range, namely $E/2 \le E_y \le E$, is put into the contribution of orbit A. In this way, we can correctly describe the

HO limit as a sum of the contributions of orbits A and B. For the Maslov index in Eq. (14), we have[13)–16), 26)] $\mu_\beta = 2\,M(n_x + n_y)$ (see also Appendix A).

Far from the bifurcations, Eq. (14), describing the contributions of the families, asymptotically approaches the SSPM result. [The function erf approaches 2 for the T orbits and 1 for the B orbits in Eq. (14).] They are identical to the Berry-Tabor trace formula for the families T and B.[5), 26)]

3.3. *Isolated orbits ($\mathcal{K} = 0$) and the Gutzwiller trace formula*

In addition to the families, there are isolated stationary points $E_y = E_y^* = E$ at the end of the classically accessible phase-space volume. These points are related to the isolated ($\mathcal{K} = 0$) periodic orbits A along the y axis. For the corresponding action variable I_x, there is a stationary point at the edge of this volume, $I_x = I_x^* = 0$. According to the transformation (4), there exists a square root singularity in I_x at $I_x = 0$, and the conjugate angle variable Θ_x' is indeterminate there. In order to remove this *spurious* singularity, we use the inverse transformation (4) from the integration variables Θ_x', I_x to the Cartesian variables x', p_x' in the double integral of Eq. (6), and then transform p_x' to p_x'' with the standard Jacobians. We now apply the ISPM in the integration over the "perpendicular" variables p_x'' and x' in order to derive the trace formula[10)] [see Eq. (6)].

As mentioned above, the stationary phase conditions (9) for the integration over the "perpendicular" momentum p_x'' imply the *closing* of the trajectory α in the spatial coordinate space, $\boldsymbol{r}' = \boldsymbol{r}'' = \boldsymbol{r}$. The action phase Φ_α (7) in the phase space trace formula (6) can be expanded in a Taylor series near the stationary point $p_x'' = p_x''{}^* = p_x^*$ up to second order, and a smooth pre-exponent amplitude is set to its value at $p_x'' = p_x^*$. As in the previous section, it is convenient to express the integral over p_x'' in terms of the error function by transforming the integration variable p_x'' to a dimensionless variable.

For the next integration over $x = x' = x''$, we can specifically write the second stationary phase condition of Eq. (9) as

$$\left(\frac{\partial \Phi_\alpha}{\partial x'} + \frac{\partial \Phi_\alpha}{\partial x''}\right)^* \equiv \left(\frac{\partial S_\alpha}{\partial x'} + \frac{\partial S_\alpha}{\partial x''}\right)^* \equiv -\left(p_x' - p_x''\right)^* = 0, \tag{17}$$

where the asterisk indicates that the function is evaluated at $x' = x'' = x^* = 0$ and $p_x'' = p_x' = p_x^* = 0$. Therefore, as explained in §3.1, we also have the closing condition for the trajectory α in momentum space $\boldsymbol{p}' = \boldsymbol{p}'' = \boldsymbol{p}$, i.e., the periodic orbit conditions which determine the isolated orbit A. Next, expanding the action $S_\alpha^*(\boldsymbol{r}', \boldsymbol{r}'', E)$ as function of $x = x' = x''$ near the *isolated* stationary point $x = x^* = 0$ to second order, we write

$$\Phi_\alpha^* \equiv S_\alpha^*(\boldsymbol{r}', \boldsymbol{r}'', E) = S_A(E) + \frac{1}{2}\mathcal{J}_\perp \left(x - x^*\right)^2, \tag{18}$$

where $S_A(E) = 2\,\pi M\,I_y(E)$ is the action along the orbit A, $I_y(E)$ is given by Eq. (2)

at $E_y = E_y^* = E$ $(I_x^* = 0)$, and M is its repetition number,

$$
\mathcal{J}_\perp = \left(\frac{\partial^2 S_\alpha}{\partial x'^{\,2}} + 2\frac{\partial^2 S_\alpha}{\partial x' \partial x''} + \frac{\partial^2 S_\alpha}{\partial x''^{\,2}} \right)^*_{x'=x''=x} = \left(-\frac{\partial p_x'}{\partial x'} - 2\frac{\partial p_x'}{\partial x''} + \frac{\partial p_x''}{\partial x''} \right)^*_{x'=x''=x} .
\tag{19}
$$

Substituting the expansion (18) of the action phase Φ_α^* into the exponent, we take the pre-exponent factor of the integral over x at the stationary point x^* determined by Eq. (17), i.e. at the *isolated periodic* orbit A, according to Eq. (9) for both x^* and p_x^* values. With the corresponding transformation of x to a new dimensionless integration variable, leading to another error function, as explained above, we finally obtain

$$
\delta g_{\text{scl}}^{(0)}(E) = \text{Re} \sum_{M \geq 1} \frac{T_A}{\pi \hbar \sqrt{|F_A|}} \, \text{erf}\left(\mathcal{Z}_A^+\right) \text{erf}\left(\mathcal{Y}_A^+\right) \exp\left[\frac{i}{\hbar} S_A(E) - \frac{i\pi}{2} \mu_A \right].
\tag{20}
$$

Here, $T_A = 2\pi/\omega_y$ is the period of the primitive orbit A (without its repetitions), F_A is the Gutzwiller stability factor,

$$
F_A = -\left(\frac{-\frac{\partial p_x'}{\partial x'} - 2\frac{\partial p_x'}{\partial x''} + \frac{\partial p_x''}{\partial x''}}{\frac{\partial p_x'}{\partial x''}} \right)_A = \text{Tr}\, M_A - 2 = -4\sin^2\left(\frac{M}{2} T_A \right),
\tag{21}
$$

where M_A is the stability matrix. The complex arguments of the error functions are given by

$$
\mathcal{Z}_A^+ = \sqrt{\frac{i\pi M K_A}{\hbar}} \, b_A^{(0)} E, \qquad \mathcal{Y}_A^+ = \sqrt{\frac{i\pi F_A}{16 M \hbar K_A}},
\tag{22}
$$

where $b_A^{(0)}$ is approximately $1/2$ (see Appendix B). In these derivations, we have expressed the finite integration limits in terms of two invariants, the curvature K_A, given in Eq. (13), and the Gutzwiller stability factor F_A, given in Eq. (21),[2),9)] for the isolated orbits A by using Eq. (4), standard Jacobian transformations, and the Liouville theorem for the conservation of the phase space volume in canonical variables. For calculations of the *asymptotic* Maslov index μ_A related to the turning and caustic points, we have used Maslov and Fedoryuk catastrophe theory[10),13)–16)] (see Appendix A), and obtain $\mu_A = 1 + 4M$. In addition, there is another phase arising from the argument of the complex error functions in Eq. (20) for the isolated orbit A, as in Eq. (14) for families. The total Maslov phase changes smoothly across the bifurcation points. Note that for integrable systems, the stability factor F_A [see Eq. (22)] causes no change in the sign at the bifurcation points, in contrast to the situation for non-integrable systems, for instance, the non-integrable Hénon-Heiles Hamiltonian.

For energies E asymptotically far from the bifurcation points E_{bif}, both error functions in Eq. (20) approach 1, and we immediately arrive at the Gutzwiller trace formula[2),4),9)] for isolated orbits A,

$$
\delta g_{\text{scl}}(E) = \frac{1}{\pi \hbar} \, \text{Re} \sum_{M \geq 1} \frac{T_A}{\sqrt{|F_A|}} \exp\left\{ \frac{i}{\hbar} S_A(E) - \frac{i\pi}{2} \mu_A \right\}.
\tag{23}
$$

We could derive the same Gutzwiller asymptotic formula (23) directly in Cartesian phase-space variables by calculating the trace integral in Eq. (6) over the perpendicular variables within the SSPM.[2),9)]

Taking the opposite limit, $E \to E_{\mathrm{bif}}$, to the bifurcation, we obtain a smooth finite result, in contrast to the divergences of the Gutzwiller trace formula, because of the exact cancellation of the singularity as $\sqrt{F_A} \to 0$ from the denominator and the second error function of the argument $\mathcal{Y}_A^+$, which behaves as $\mathcal{Y}_A^+ \propto \sqrt{F_A} \to 0$, in Eq. (20). Another singularity of the SSPM due to the infinite curvature K_A in the limit to the barrier energy $E \to E_b$ (an infinitely dense bifurcation point or separatrix) is removed similarly, due to the finite limits (22) in the ISPM oscillating level density (20) for isolated orbits, and, moreover, it becomes zero there.

Note that the contribution of the isolated orbits A, given by Eq. (20), differs from Eq. (11) that is similar to the Poisson summation trace formula, because of the second error function $\mathrm{erf}(\mathcal{Y}_A^+)$, which seems to be beyond the approximation based on the assumption in Ref. 6) that the trace integrand in Eq. (10) is independent of the angle variables. The equivalent derivations of the Gutzwiller trace formula, asymptotically from the ISPM trace formula (20) for the isolated orbits A and directly from the phase-space trace formula (6) using the SSPM, seem to be more consistent with each other than with another SSPM approach based on the endpoint contributions to the EBK Poisson summation trace formula.[26)] Note also that the ISPM trace formula (20) for isolated orbits A is more general than these endpoint contributions, because it is valid near the bifurcations.

3.4. *Total trace formula*

The total ISPM trace formula of the level density $g_{\mathrm{scl}}(E)$ for the IHH Hamiltonian is given by the sum over the contributions of the (extended) Thomas-Fermi average density[9)] and the contributions of all periodic orbits, including the families $\delta g_{\mathrm{scl}}^{(1)}(E)$ of Eq. (14) and the isolated ones $\delta g_{\mathrm{scl}}^{(0)}(E)$ of Eq. (20):

$$g_{\mathrm{scl}}(E) = g_{\mathrm{TF}}(E) + \delta g_{\mathrm{scl}}^{(1)}(E) + \delta g_{\mathrm{scl}}^{(0)}(E)$$
$$= g_{\mathrm{TF}}(E) + \mathrm{Re} \sum_{\beta} A_\beta(E) \exp\left[\frac{i}{\hbar} S_\beta(E) - \frac{i\pi}{2}\mu_\beta\right]. \qquad (24)$$

This trace formula has the correct finite asymptotic limits to the SSPM, the Berry and Tabor result[5)] for the families B and T, and Gutzwiller trace formula[2)] for isolated orbits A as well as to the HO trace formula (see Appendix B and Refs. 9) and 26)). The ISPM contribution (14) of the family B converges to half of the HO trace formula. As shown in Appendix B, its other half is obtained as the limit of the ISPM contribution (20) of the isolated orbits A.

The level density $g_{\mathrm{scl}}(E)$ coarse grained using a Gaussian weight function with averaging parameter γ can also be expressed analytically as a sum over periodic orbits β, as in Eq. (24), but with an additional factor $\exp[-(MT_\beta\gamma/\hbar)^2]$ for each term.[4),9)]

The semiclassical periodic-orbit expansion for the Strutinsky shell structure en-

ergies is given by[4),9),10),12)]

$$\delta E(N) = 2 \sum_{\beta} \left(\hbar / M T_{\beta}(E_F) \right)^2 \delta g_{\beta}(E_F), \quad \text{with} \quad N = 2 \int_0^{E_F} dE\, g(E), \qquad (25)$$

where δg_{β} is the β component of the periodic-orbit sum in Eq. (24), $\delta g = \delta g^{(1)} + \delta g^{(0)} = \sum_{\beta} \delta g_{\beta}$. The spin degeneracy is explicitly taken into account by the factor of 2. Note that the contribution of long periodic orbits to the energies is suppressed due to the factor of $(\hbar / M T_{\beta})^2$.

§4. Comparison with quantum mechanics

We now compare the ISPM level densities and shell structure energies with those of quantum mechanics. Figures 3 and 4 display the ISPM and SSPM complex amplitudes A_{β} [the moduli $|A_{\beta}|$ and their arguments, including the Maslov index μ_{β} through the total Maslov phase $\mu_{\beta}(E) = \mu_{\beta} - 2\arg(A_{\beta}(E))/\pi$] for the families B $(1,1)$ and T $(20,19)$. The results of the Poisson summation trace formula (11), derived using a more exact trace integration with the limits from 0 to $b_{\beta}^{(1)}E$ of Eq. (16) related to the family B are also plotted. As seen from the upper panel of Fig. 3, the ISPM amplitude $|A_{\text{B}}|$ for the family B has the correct limits to a half of the HO amplitude A_{HO} at $E = 0$ and to the Berry and Tabor (SSPM) asymptotics[5),26)] for larger E. Also note that there is good agreement with the Poisson (P,B) results, which improves as the energy decreases. The other half of the HO amplitude, A_{HO}, is provided by the ISPM amplitude (20) for the isolated orbits A in the HO limit $E \to 0$. The latter amplitude is also in good agreement with that of the Gutzwiller trace formula[2),9)] for energies E asymptotically far from the bifurcation energy $E_{\text{bif}} = 0$. Note that we have *enhancement* of the amplitude of family B (ISP,B and P,B) slightly to the right of the bifurcation point $E = 0$ also for the orbit A. This enhancement is related to a local change of the degeneracy (symmetry) parameter by two units for the orbits A and by one unit for the family B in the HO limit. Note that the ISPM amplitude $|A|$ for the orbit A becomes zero at the barrier energy $E = E_b$, in contrast to the divergence of the SSPM. The lower panel reveals a similarly good agreement of the ISPM total Maslov phases $\mu_{\beta}(E)$ with their asymptotic SSPM and more exact Poisson trace formula (11).

In Fig. 4, there are many more bifurcations, which become infinitely dense at the barrier energy E_b, but there is also nice agreement with the SSPM and Poisson (P,T) approximations for the ISPM amplitude $|A_{\beta}|$ and Maslov phases $\mu_{\beta}(E)$. This figure is reminiscent of the bifurcation scenarios for hyperbolic orbits bifurcated from repeated short diameters in elliptic billiard systems.[10)] As in elliptic billiards, we have enhancement of the amplitude for the family slightly to the right of the bifurcation point, but the ISPM amplitude of the orbit A ($n_y = 19$) has a maximum exactly at the bifurcation. As seen in Fig. 4, all divergences of the SSPM density amplitudes are removed by the ISPM. In particular, the ISPM amplitude $|A|$ for the orbit A tends to zero in the barrier energy limit, $E \to E_b$. We also emphasize that there is enhancement of the amplitude due to the increase of the symmetry
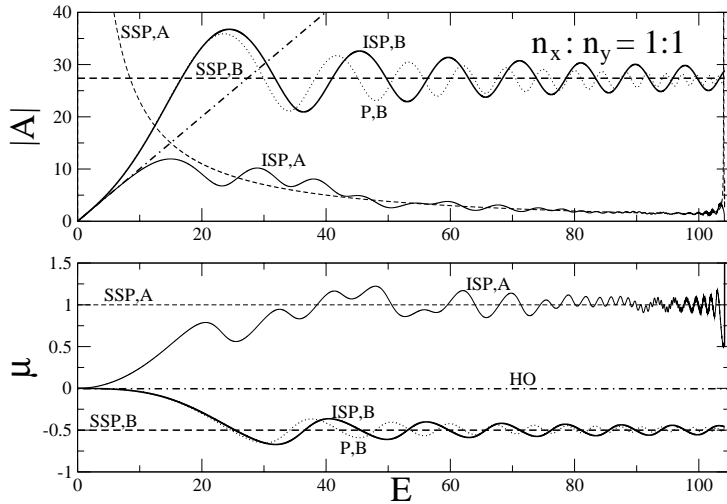
Fig. 3. Amplitudes $|A_\beta(E)|$ and total Maslov phases $\mu_\beta(E)$ for bifurcation of the primitive ($n_y = 1$) orbit A into itself and the family B $(1,1)$, $\epsilon = 0.04$. The thin solid line (ISP,A) is the ISPM result for the isolated orbits A, and the thick solid line (ISP,B) represents the family B; the dashed lines (SSP,A) and (SSP,B) represent their SSPM asymptotics, respectively. The dash-dotted lines indicate $|A_\beta|/2$ and the Maslov phase for the $(1,1)$ component (HO) of the HO trace formula. The dotted line (P,B) represents the B component of the Poisson summation trace formula (11).
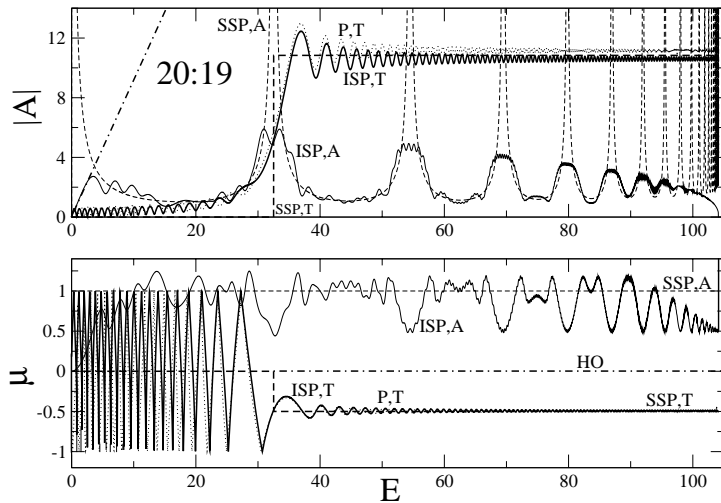
Fig. 4. The same as Fig. 3, but for the family T $(20, 19)$.

parameter $\mathcal{K}$ by 1 for orbits A locally near the bifurcation point and slightly to the right of the bifurcation for the corresponding bifurcating family T.

Semiclassical and quantum level densities for $\epsilon = 0.04$, 0.08 and 0.1 are compared in Figs. 5, 6 and 7, respectively. Our ISPM semiclassical trace formula, (24), is in good agreement with the quantum densities for both the gross shell ($\gamma = 0.1$) and
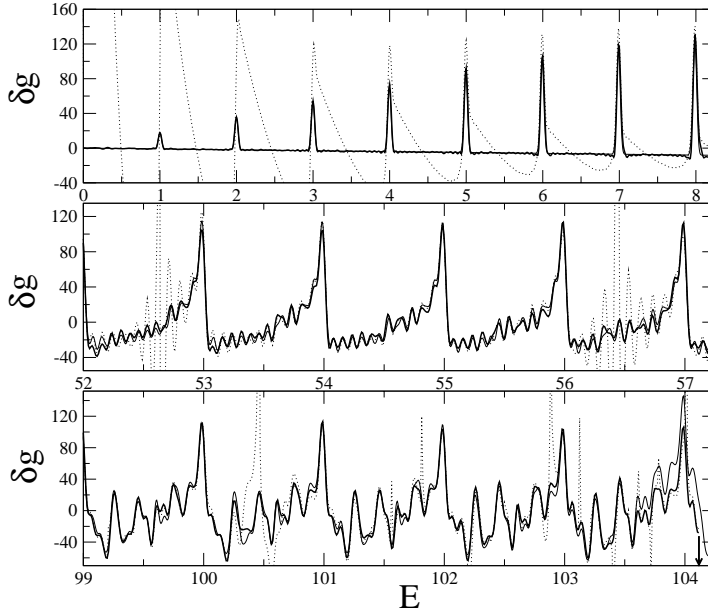
Fig. 5. Comparison of oscillating level densities $\delta g(E)$ coarse grained with the averaging parameter $\gamma = 0.03$ (rather fine shell structures) for $\epsilon = 0.04$. The thin solid, thick solid and dotted curves represent the quantum, ISPM and SSPM results. The arrow located on the right side of the bottom panel indicates the barrier energy.

finer ($\gamma = 0.03$) structures. In order to obtain convergence of the POT sums in Eq. (24) with the averaging parameter $\gamma = 0.03$, we have to include Mn_x and Mn_y up to the maximal value 16, which is a factor of two larger than in the case $\gamma = 0.1$.

We also have good asymptotics to SSPM between successive bifurcations, as well as in the HO limit $E \to 0$, for all values of ϵ. For the gross shell structure ($\gamma = 0.1$), even the SSPM densities are in good agreement with the quantum results almost everywhere, except in small regions near the bifurcations of the short periodic orbits entering into the trace sum. For smaller γ, significantly longer periodic orbits enter into the trace sum, and they experience bifurcations very frequently. (See the frequent divergences of the SSPM density in Figs. 5–7.) In such cases, as compared with the quantum results, the ISPM becomes a much better approximation than the SSPM over almost the entire energy region between successive bifurcations.

Figures 8–10 compare the semiclassical and quantum shell structure energies δE. The SSPM and ISPM energies are given by Eq. (25), and the quantum results are obtained using the Strutinsky shell correction method (see Appendix C for details). As seen from these figures, the ISPM shell structure energies are also in nice agreement with the quantum results, exactly up to the barrier energy. It is seen that the ISPM significantly improves the SSPM, as in the case of oscillating level densities, where the SSPM suffers divergences due to the bifurcations. We also find that there are good asymptotics to the HO and SSPM limits of the ISPM shell structure energies, except for such divergences. Increasing the particle number N and the "deformation" parameter ϵ, we obtain a more dense bifurcation cascade. However,
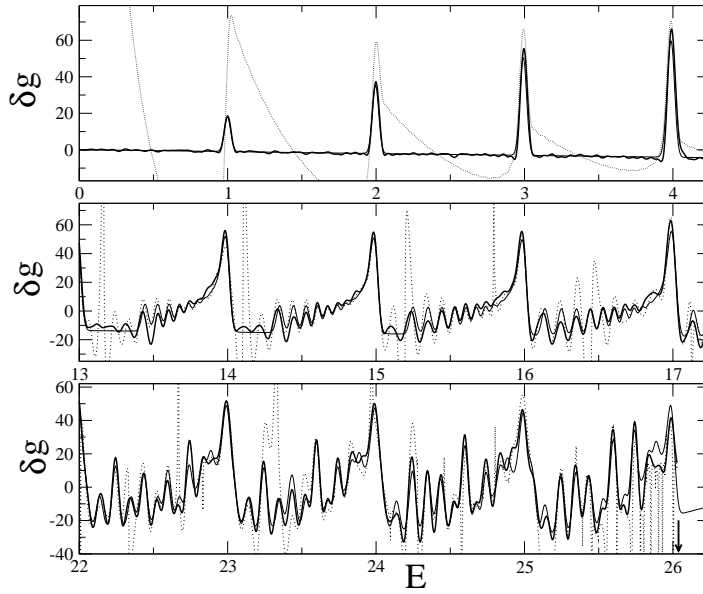
Fig. 6.   The same as in Fig. 5, but for $\epsilon = 0.08$.
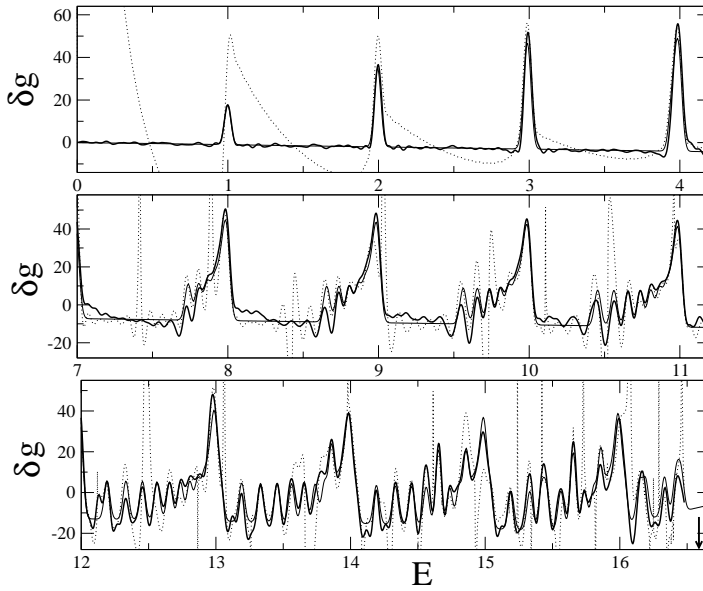
Fig. 7.   The same as in Fig. 5, but for $\epsilon = 0.1$.

the ISPM still solves the bifurcation problems well enough for calculations of the shell structure energies as well as the averaged level densities.
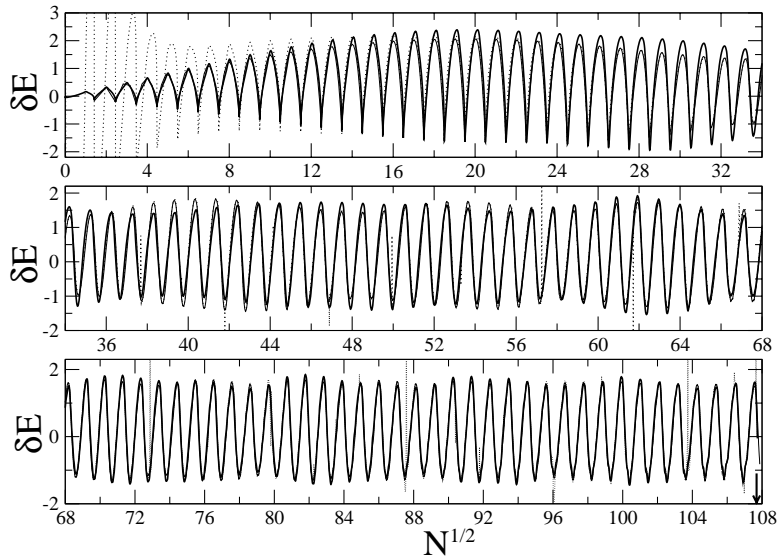
Fig. 8. The shell structure energies δE as functions of square root of the particle number, $N^{1/2}$, for the "deformation" parameter value $\epsilon = 0.04$. Various curves have the same meanings as in Figs. 5–7.

§5. Conclusions

We derived the semiclassical trace formula (24) for the integrable version of the Hénon-Helies Hamiltonian using the ISPM within the EGA, starting from the general phase-space trace formula for the level density (6). This formula was obtained as the periodic-orbit sum of the *separate* contributions of families and isolated periodic orbits related to continuous and isolated stationary points in the "perpendicular" phase-space variables, respectively.

The ISPM trace formula for the single-particle level density (24) *averaged analytically* for gross-to-fine shell structures and the corresponding expressions for *shell structure energies* can be applied to *any dense* cascade of bifurcations near the potential barrier. The ISPM trace formulas (24) and (25) are *continuous through all symmetry-breaking points*, including the known harmonic oscillator limit, and all other bifurcations up to the barrier energy. They also have the correct and straightforward SSPM Berry-Tabor and Gutzwiller asymptotics far from the bifurcations in the case that they exist.

We point out that the only *stationary-phase points* were taken into account in the ISPM derivations of the trace formula (24). In our approach, the endpoints, which belong to the boundary of the phase-space volume occupied by classical trajectories, are the stationary-phase points corresponding to the B family and the isolated periodic orbit A (with repetitions). The latter is regarded as the limit value of the infinite sequence of internal stationary points found from the resonance equation (5). Thus, the complete trace formula for any integrable system can be obtained as a sum of only stationary points if we take into account all of them, including those related to
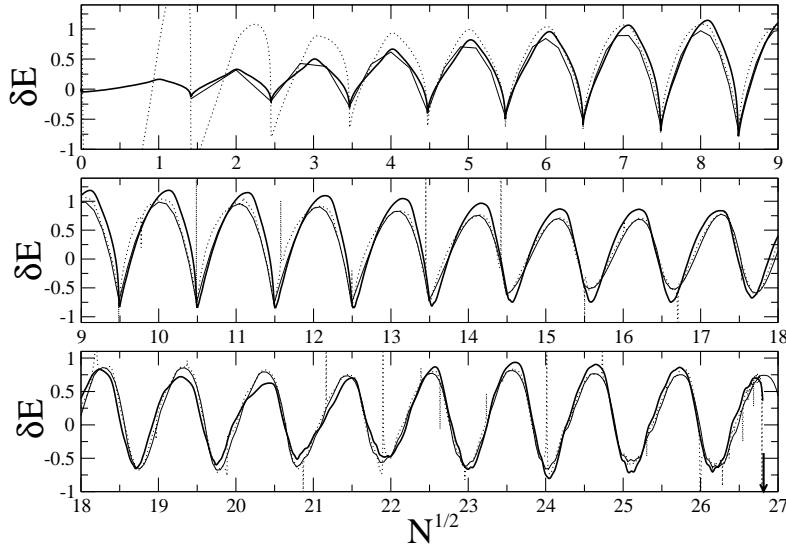
Fig. 9.   The same as in Fig. 8, but for $\epsilon = 0.08$.
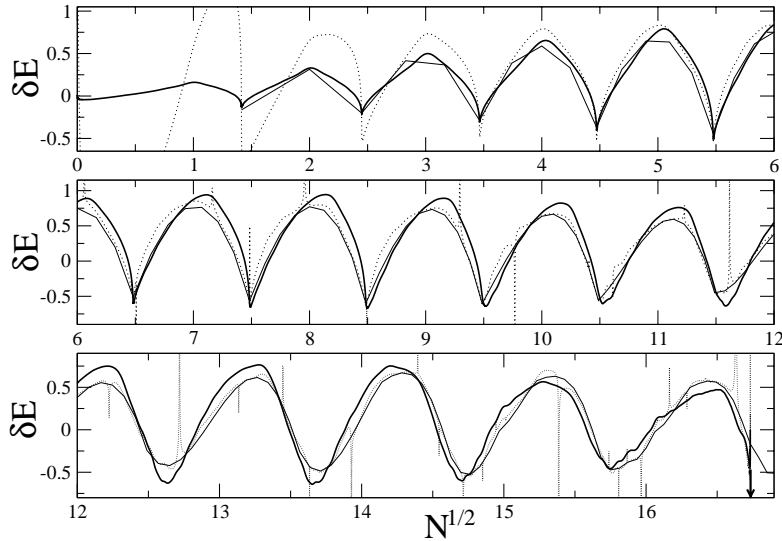
Fig. 10.   The same as in Fig. 8, but for $\epsilon = 0.1$.

long-time orbits.[38] Note also that some other $\hbar$ end corrections are included already in the periodic orbit sums (14) for families and (20) for isolated orbits through the finite limits in the error integrals as the stationary-point contributions within the same ISPM.

The contribution of the isolated orbits A, given by Eq. (20), is an *additional* term to Eq. (14) for the families B and T. The latter was derived in the ISPM from Eq. (11), which is reminiscent of the Poisson summation trace formula of the EBK with respect to its analytical structure, but is actually different due to the restrictions

on the summation integers. These two ISPM trace formulas, Eq. (20) for A and Eq. (14) for B and T orbits, are very different, due to the second error function of the argument proportional to the Gutzwiller stability factor, $\sqrt{F_A}$, in Eq. (20). The ISPM trace formula (20) for the isolated orbits can be applied everywhere, including all bifurcation points and the separatrix (potential barrier), and therefore, it is more general than the Gutzwiller trace formula.[2] In the ISPM, we found enhancement of the shell-structure density amplitudes for both isolated and family orbits near the bifurcation points which is related to the local increase of their degeneracy parameter $\mathcal{K}$. This can be understood by considering a rather general arguments of symmetry-breaking, as in the case of elliptic and spheroidal box potentials.[10]–[12]

Our results for the coarse-grained level densities for several typical values of the "deformation" parameter $\epsilon \lesssim 0.1$ and the corresponding shell structure energies are in good agreement with the quantum results. As ϵ increases, bifurcations become more dense, but nevertheless, the good agreement of the ISPM densities with the quantum results is maintained. From this comparison, in the case of finer shell-structure averaging, we found large energy regions, with widths on the order of a distance between successive bifurcations, where the ISPM is far superior to the SSPM. The ISPM is generally applicable to any integrable system and can be helpful also for non-integrable systems, such as the famous Hénon-Heiles Hamiltonian.

Appendix A
—— *Catastrophe Theory* ——

In this appendix we outline catastrophe theory, basically following the presentation of Refs. 13)–16), with the main focus on the points related to our bifurcation problem of the ISPM. The catastrophe integral $I(\alpha, \kappa)$,

$$I(\alpha, \kappa) = \int_{x_-}^{x_+} dx A(x, \alpha) \exp\left[i \kappa \Phi(x, \alpha)\right], \tag{A·1}$$

is regarded as a function of two dimensionless parameters, a small parameter α in the Hamiltonian and a large one κ related to $1/\hbar$ in the POT. The limits of integration $x_\pm$ are some *finite* values. We assume that the integral (A·1) has the simplest (first

order) caustic catastrophe point $x^*(\alpha)$ at $\alpha = 0$ defined as

$$\left(\frac{\partial \Phi}{\partial x}\right)^* = 0, \qquad \left(\frac{\partial^2 \Phi}{\partial x^2}\right)^* = 0, \qquad \left(\frac{\partial^3 \Phi}{\partial x^3}\right)^* = \mathcal{O}\left(\alpha^0\right), \qquad (\text{A·2})$$

where the asterisk means that the derivatives are taken at $x = x^*(0)$. The mixed derivative $(\partial^2 \Phi/\partial x \partial \alpha)^*$ is assumed to be of zeroth order in α, like the third derivative in Eq. (A·2). In order to remove the degeneracy of the two simple stationary points and obtain the one caustic point given by Eq. (A·2), let us consider a small perturbation of the catastrophe integral $I(\alpha, \kappa)$ given in Eq. (A·1) by slightly altering α, and hence the phase function $\Phi(x, \alpha)$ and the amplitude $A(x, \alpha)$, near the caustic point $\alpha = 0$. For *any small nonzero* α, we first consider the expansion of the action $\Phi(x, \alpha)$ in a Taylor series,

$$\Phi(x, \alpha) = \Phi^* + \frac{1}{2}\left(\frac{\partial^2 \Phi}{\partial x^2}\right)^* (x - x^*)^2 + \frac{1}{6}\left(\frac{\partial^3 \Phi}{\partial x^3}\right)^* (x - x^*)^3 + \cdots, \qquad (\text{A·3})$$

near the stationary point $x^*(\alpha)$. The star in this equation means that the derivatives are taken at $x = x^*(\alpha)$, $\Phi^* = \Phi(x^*, \alpha)$. For a small perturbation (i.e., small α), the second derivative in Eq. (A·3) is nonzero, but small in the case of the simplest caustic point (A·2). In particular, one may simply consider this derivative as the parameter α. The third derivative of the phase Φ does not become zero near the caustic point $\alpha = 0$ for any considered α. The amplitude $A(x, \alpha)$ is also expanded near the stationary point $x^*(\alpha)$, like the phase $\Phi(x, \alpha)$ in Eq. (A·3). Here, we assume that $A(x^*, \alpha)$ has *finite nonzero* limit $\alpha \to 0$.

For the asymptotic expansion $\kappa \to \infty$, we can now truncate the expansion (A·3) for the phase $\Phi(x, \alpha)$ and the corresponding one for the amplitude $A(x, \alpha)$ at the third and zeroth orders, respectively, keeping a *small nonzero* α, and substitute them into the catastrophe integral $I(\alpha)$ (A·1). Then, using the *linear transformation* of the coordinates,

$$x = x^* + \lambda_0 + \lambda z, \qquad \lambda_0 = -\frac{(\partial^2 \Phi/\partial x^2)^*}{(\partial^3 \Phi/\partial x^3)^*}, \qquad \lambda = \left[\frac{\kappa}{2}\left(\frac{\partial^3 \Phi}{\partial x^3}\right)^*\right]^{-1/3}, \qquad (\text{A·4})$$

one can reduce the catastrophe integral (A·1) to the analytical form

$$I(\alpha, \kappa) = \pi \lambda A^* \exp\left(i\,\kappa\,\Phi^* + \frac{2i}{3}\,w^{3/2}\right) [\text{Ai}(-w, z_-, z_+) + i\,\text{Gi}(-w, z_-, z_+)], \qquad (\text{A·5})$$

with the extended Airy and Gairy integrals within finite limits:

$$\begin{Bmatrix} \text{Ai} \\ \text{Gi} \end{Bmatrix}(-w, z_1, z_2) = \frac{1}{\pi}\int_{z_1}^{z_2} dz \begin{Bmatrix} \cos \\ \sin \end{Bmatrix}\left(-wz + \frac{z^3}{3}\right). \qquad (\text{A·6})$$

The argument w of these functions and the finite limits $z_\pm$ in Eq. (A·5) are given by

$$w = \left(\frac{\kappa}{2}\right)^{2/3}\left[\frac{(\partial^2 \Phi/\partial x^2)^2}{(\partial^3 \Phi/\partial x^3)^{4/3}}\right]^* > 0, \qquad z_\pm = \lambda^{-1}(x_\pm - x^*) + \sqrt{w}. \qquad (\text{A·7})$$

As seen from the cubic form of the phase in Eq. (A·6), the caustic point can be considered a crossing point of the two simple *close* stationary curves, $z_\pm^*(\alpha) = \pm\sqrt{w}$, in the new variable z of Eq. (A·4) for any *small nonzero* α, which merge into one caustic point $z_\pm^*(\alpha) \to 0$, given in Eq. (A·2), in the limit $\alpha \to 0$. The final result is the sum of the contributions of these stationary points. Note that according to the first equation in Eq. (A·7), the value of w becomes *large* for *any fixed nonzero* α as $\kappa \to \infty$. Nevertheless, it is *small* for a *large fixed finite nonzero* κ when α is *small*. However, we can may consider both cases using the same extended trace formula (A·5), because the two parameters α and κ appear in Eq. (A·7) in terms of one parameter, w.

For instance, for any small nonzero α, we can find a κ sufficiently large that w can be large, and the two abovementioned stationary points, $z_\pm^*(\alpha)$, are *separated* sufficiently well. For definiteness, it is enough to consider $z_+ > 0$ and $z_- < 0$ and split the integration interval into two parts, from z_- to 0 and from 0 to z_+ in order to separate the negative and positive internal stationary points, $-\sqrt{w}$ and $\sqrt{w}$, respectively. For the second integral over positive z the upper integration limit z_+ can be extended to *infinity*, as in SSPM, because $z_+ \propto \kappa^{1/3} \gg 1$ and $z_+ \gg z_+^* = \sqrt{w}$ for small α [see Eq. (A·7)]. Within this approximation, one can use the asymptotics[37] of the standard complete Airy and Gairy functions, $Ai(-w)$ and $Gi(-w)$, which correspond to the limits $z_1 = z_- = 0$ and $z_2 = z_+ = \infty$ in Eq. (A·6) for $w \to \infty$ in Eq. (A·5). In this way, asymptotically far from the caustic point (A·2), we obtain the same result as we would with the standard second-order expansion of the phase Φ at a simple [with finite $(\partial^2\Phi/\partial x^2)^*$] stationary point x^* but with a shift of the phase Φ by $-\pi/2$. The other part of the integral over the negative values of z, which includes the negative stationary point, can obviously be considered in an analogous manner with the change of the integration variable $z \to -z$. Thus, the famous Maslov theorem[14] regarding the shift of the action phase Φ by $-\pi/2$ (Maslov index) at each simple caustic point (A·2) of the classical trajectory (in particular, the periodic orbit) in SSPM can be immediately proved by using Fedoryuk's method formulated in the first paper listed in Ref. 13). For the case of the *turning point*, we have the conditions (A·2), replacing zero by ∞ in the second equation. In this case Fedoryuk used the elegant linear coordinate transformation which reduces such singularity to the caustic one, i.e. the second derivative of the phase Φ in a new variable becomes zero [see the second paper in Ref. 13)]. Therefore, we obtain the same shift of $-\pi/2$ at each simplest turning point along the classical trajectory; i.e., the next part of Maslov theorem[14] concerning the Maslov index generated by such a turning critical point is also proved within the same catastrophe theory of Fedoryuk.[13]

We may also find such a κ for any small nonzero α for which w is *small*, but the two stationary points for the action in the catastrophe integral (A·5) are *separated* by a sufficient amount. We use this in the ISPM in order to obtain convergence of expansions like Eq. (A·3) to second order and a sum over separate contributions of different kinds of isolated and family orbits, as in the derivation of the Maslov theorem, but within *finite* limits of integration. The latter is important because the critical bifurcation point is formally a specific caustic which, however, belongs to the

boundary of the classical motion (see the main text).

Appendix B
—— Harmonic Oscillator Limit ——

Let us consider the HO limit, $E \to 0$, for the trace formula (24) ($\omega_y \to \omega_x = 1$). This limit is a specific bifurcation, $E_{\text{bif}} = E_y^* = 0$, where the two parameter ($\mathcal{K} = 2$) families of the HO are bifurcated into the one-parameter ($\mathcal{K} = 1$) family B as the symmetry parameter $\mathcal{K}$ decreases by one unit and the isolated ($\mathcal{K} = 0$) orbits A as $\mathcal{K}$ decreases by two units. Taking the limit $E \to 0$ of the density amplitudes A_β for the family B in Eq. (14) and isolated orbits A of Eq. (20), we obtain ($n_y = 1$)

$$A_{\text{B}}^{(1)} = \frac{T_\beta}{\pi \sqrt{-iM\hbar^3 K_\beta}} \; \text{erf}\left(\mathcal{Z}_\beta^-, \mathcal{Z}_\beta^+\right) \to \frac{2}{\hbar^2} b_{\text{B}}^{(1)} E,$$

$$A_{\text{A}}^{(0)} = \frac{T_A}{\pi \, \hbar \, \sqrt{|F_A|}} \text{erf}\left(\mathcal{Z}_A^+\right) \text{erf}\left(\mathcal{Y}_A^+\right) \to \frac{2}{\hbar^2} b_{\text{A}}^{(0)} E. \tag{B·1}$$

We used the expressions in Eqs. (15) and (22) for the finite limits of the corresponding error functions and expanded these functions in power series of small arguments. The stability factor $\sqrt{F_A}$ in the denominator of the ISPM isolated-A-orbit trace formula Eq. (20) goes to zero in the HO limit, as for all other bifurcations. However, this singularity, which leads to the divergence of the standard SPM Gutzwiller trace formula, is canceled in the ISPM by the same $\sqrt{F_A}$ coming from the linear term of the first-order expansion of the error function of the argument $\mathcal{Y}_A^+ \propto \sqrt{F_A} \to 0$ ($F_A/K_A \to 0$). The curvatures K_B and K_A also become zero HO curvature in this limit. However, there are similar cancellations of these singularities ($\sqrt{K_\beta} \to 0$) from the denominators and numerators if we also take into account the linear terms in expansion of the error functions in Eqs. (14) and (15) for family B and in Eqs. (20) and (22) for the isolated orbit A. The action S_β for both kinds of orbits, A and B, tends to the same action S_{HO} for the HO orbits: $S_B \to S_A \to S_{\text{HO}} = 2\pi M E/\hbar$. Thus, for the total oscillating level densities of Eq. (24), we obtain

$$\delta g(E) \to \delta g_{\text{B}}^{(1)}(E) + \delta g_{\text{A}}^{(0)}(E) \to \frac{2}{\hbar^2} \left(b_{\text{B}}^{(1)} + b_{\text{A}}^{(0)}\right) \sum_{M=1}^{\infty} \cos\left(\frac{M}{\hbar} 2\pi E\right)$$

$$= \frac{2E}{\hbar^2} \sum_{M=1}^{\infty} \cos\left(\frac{M}{\hbar} 2\pi E\right). \tag{B·2}$$

The second line here was obtained using the approximations appearing in Eq. (16) for the integration boundary coefficient $b_{\text{B}}^{(1)}$, in the B component of the family trace formula $\delta g_{\text{scl}}^{(1)}$ given in Eq. (14), and $1/2$ for $b_{\text{A}}^{(0)}$ in the finite limit Eq. (22) of the isolated-A-orbit contribution $\delta g_{\text{scl}}^{(0)}$ appearing in Eq. (20). Note that in the derivation of the HO limit, we used the specific boundaries $b_B^{(1)}$ of Eq. (16) and $b_A^{(0)} = 1/2$ only in the last transformation of Eq. (B·2).

These limits and orbits themselves are coupled in principle at the HO bifurcation $E = 0$ into one two-parameter family of the HO and cannot be distinguished in

this limit. However, we can formally separate them in this limit by assuming the symmetry of these two kinds of orbits A and B at $E = 0$ and connecting them with the different tori parts occupied by the two-parameter family manifold. It is natural to connect B orbits with the tori part related to the energies E_y from 0 to $E/2$ and A orbits with another part from $E/2$ to E, because the B families correspond to the end-stationary point, $E_y = E_y^* = 0$, and A orbits to the other end-stationary point, $E_y = E_y^* = E$, for all energies up to the barrier energy E_b.

For B families, we can now evaluate the transition region from its stationary (bifurcation) point, $E_y^* = E_{\mathrm{bif}} = 0$, up to the asymptotic region far from this HO bifurcation by using the second-order expansion of the action phase Φ_α within the ISPM which leads to a Gaussian form with the dispersion Δ_{B} [see the second relation in Eq. (16)]. Because of the relative smallness of Δ_{B} for the B families in the semiclassical limit, $\hbar \to 0$, the upper limit of the ISPM integration for the B family contribution changes sharply from $E/2$ to E as the energy E is increased from zero to the barrier value E_b within a small dispersion $2\Delta_{\mathrm{B}}$. Therefore, this limit can be approximated, for instance, as in Eq. (16). For the boundaries Eq. (22) of the isolated A orbits, the lower limit of integration can be approximated simply by the constant $E/2$, independently of the energy E, because the dispersion (transition region) $\Delta_{\mathrm{A}} = 1/\sqrt{\pi M n_y K_{\mathrm{A}}/\hbar}$ ($K_{\mathrm{A}} = K_{\mathrm{B}}$ at $E_y = 0$) decreases as the energy increases, $K_{\mathrm{A}} > K_{\mathrm{B}}$, and the stationary point for the isolated A orbits is the endpoint $E_y^* = E$, which gives the main contribution to the trace integral. The integration limits for the Θ_x' variable can be approximated in a similar way.

Appendix C
—— *Application of the Strutinsky Method to a Finite-Depth Potential* ——

It is well known that a direct application of the Strutinsky shell correction method fails in a threshold region because there exists no clear plateau.[33),39),40)] The main reason for this problem is the absence of a sufficient number of discrete levels when the Fermi level is close to the continuum, and there is thus a rapid change of the average level density. Therefore, in order to calculate the shell structure energy δE up to the threshold energy E_b, we need discrete levels located approximately a few major shells above the threshold.

One of the previous approaches to overcome this problem is based on accounting for resonance states in the continuum, for instance, within the Green function formalism.[32),41),42)] However, we use the simpler method of discretizing the continuum by introducing an infinite well at a suitably far distance from the barrier. We modify the IHH potential as

$$V(x,y) = \frac{1}{2}x^2 + V_y(y), \qquad V_y(y) = \begin{cases} \dfrac{1}{2}y^2 - \dfrac{\epsilon}{3}y^3, & y \le y_b = \dfrac{1}{\epsilon}, \\[2mm] E_b = \dfrac{1}{6\epsilon^2}, & y_b < y \le y_w = 1.2y_b, \\[2mm] \infty, & y_w < y. \end{cases} \tag{C.1}$$

This modification leads to only very small changes in the energy levels below the

threshold, and it has almost no effect on the shell structure energy in this energy region. We next transform the single-particle spectrum $\{E_i\}$ $(i = 1, 2, 3, \cdots)$ to one whose average level density is a simple function $f(w)$:

$$\tilde{g}(E)dE = f(w)dw. \tag{C·2}$$

For $f(w) = w$, we obtain new levels $\{w_i\}$ as

$$w_i^2 = w_{i-1}^2 + 2 \int_{E_{i-1}}^{E_i} g_{\mathrm{TF}}(E)dE \quad (i \geq 1), \qquad w_0 = E_0 = 0, \tag{C·3}$$

where we have used the Thomas-Fermi approximation[9] $g_{\mathrm{TF}}(E)$ for the average density $\tilde{g}(E)$. Then, we apply the Strutinsky method[33] to the new spectrum $\{w_i\}$ and calculate the shell occupation numbers δn_i. Finally, the shell structure energy δE is obtained as

$$\delta E = 2 \sum_i E_i \delta n_i. \tag{C·4}$$

In this procedure, we can always obtain a clear plateau for the stability of δE as a function of a parameter of the smoothing of the occupation numbers n_i.

Note that a similar method with the transformation (C·2) for the case in which w is related to the particle number is suggested in Refs. 39) and 40). The method based on the transformation (C·2) is general and can be applied to the single-particle spectra of any potentials with finite depth. Moreover, it is much simpler than the methods mentioned above.

References

1) M. C. Gutzwiller, J. Math. Phys. **12** (1971), 343, and earlier references quoted therein.
2) M. C. Gutzwiller, *Chaos in Classical and Quantum Mechanics* (Springer-Verlag, New York, 1990).
3) R. B. Balian and C. Bloch, Ann. of Phys. **69** (1972), 76.
4) V. M. Strutinsky, Nukleonika **20** (1975), 679.
   V. M. Strutinsky and A. G. Magner, Sov. Phys. Part. Nucl. **7** (1977), 138.
5) M. V. Berry and M. Tabor, Proc. R. Soc. London A **349** (1976), 101.
6) M. V. Berry and M. Tabor, J. of Phys. A **10** (1977), 371.
7) V. M. Strutinsky, A. G. Magner, S. R. Ofengenden and T. Døssing, Z. Phys. A **283** (1977), 269.
8) S. C. Creagh and R. G. Littlejohn, Phys. Rev. A **44** (1990), 836; J. of Phys. A **25** (1992), 1643.
9) M. Brack and R. K. Bhaduri, *Semiclassical Physics* (Addison-Wesley Reading, 1997).
10) A. G. Magner, S. N. Fedotkin, K. Arita, K. Matsuyanagi, T. Misu, T. Schachner and M. Brack, Prog. Theor. Phys. **102** (1999), 551.
11) A. G. Magner, S. N. Fedotkin, K. Arita, K. Matsuyanagi and M. Brack, Phys. Rev. E **63** (2001), 065201(R).
12) A. G. Magner, K. Arita, S. N. Fedotkin and K. Matsuyanagi, Prog. Theor. Phys. **108** (2002), 853.
13) M. V. Fedoryuk, Sov. J. Comp. Math. and Math. Phys. **4** (1964), 671; ibid. **10** (1970), 286.
14) V. P. Maslov, Theor. Math. Phys. **2** (1970), 30.
15) M. V. Fedoryuk, *Saddle-point method* (Nauka, Moscow, 1977, in Russian).
16) M. V. Fedoryuk, *Asymptotics: Integrals and sums* (Nauka, Moscow, 1987, in Russian).
17) C. Chester, B. Friedmann and F. Ursell, Proc. Cambridge Philos. Soc. **53** (1957), 599.

18) S. Tomsovic, M. Grinberg and D. Ullmo, Phys. Rev. Lett. **75** (1995), 4346.
    D. Ullmo, M. Grinberg and S. Tomsovic, Phys. Rev. E **54** (1996), 136.
19) M. Sieber, J. of Phys. A **30** (1997), 4563.
20) P. Meier, M. Brack and C. Creagh, Z. Phys. D **41** (1997), 281.
21) H. Schomerus and M. Sieber, J. of Phys. A **30** (1997), 4537.
22) M. Sieber and H. Schomerus, J. of Phys. A **31** (1998), 165.
23) H. Schomerus, J. of Phys. A **31** (1998), 4167.
24) M. Brack, P. Meier and K. Tanaka, J. of Phys. A **32** (1999), 331.
25) M. Brack, S. Fedotkin, A. G. Magner and M. Mehta, J. of Phys. A **36** (2003), 1095.
26) J. Kaidel and M. Brack, Phys. Rev. E **70** (2004), 016206.
27) A. M. Ozorio de Almeida and J. H. Hannay, J. of Phys. A **20** (1987), 5873.
28) A. M. Ozorio de Almeida, *Hamiltonian Systems: Chaos and Quantization* (Cambridge University Press, Cambridge, 1988).
29) S. C. Creagh, Ann. of Phys. **248** (1996), 60.
30) M. Brack, Foundations of Physics **31** (2001), 209.
31) M. Brack, M. Mehta and K. Tanaka, J. of Phys. A **34** (2001), 8199.
32) J. Kaidel, P. Winkler and M. Brack, Phys. Rev. E **70** (2004), 066208.
33) V. M. Strutinsky, Nucl. Phys. A **95** (1967), 420; ibid. **122** (1968), 1.
34) M. Brack, private communications (2005).
35) L. D. Landau and E. M. Lifshits, *Mechanics*, Third edition (Pergamon Press Ltd., 1976).
36) A. D. Bruno, Math. USSR Sbornik **12** (1970), 271; Inst. Prikl. Mat. Akad. Nauk SSSR. Preprint No. 18 (Moskow, 1972, in Russian).
37) M. Abramowitz and I. A. Stegun, *Handbook of mathematical functions* (Dover publications INC., New York, 1964).
38) A. M. Ozorio de Almeida, C. H. Lewkopf and S. Tomsovic, J. of Phys. A **35** (2002), 10629.
39) F. A. Ivanyuk and V. M. Strutinsky, Z. Phys. A **290** (1979), 107.
40) F. A. Ivanyuk, Z. Phys. A **316** (1984), 237.
41) T. Vertse, A. T. Kruppa and W. Nazarewicz, Phys. Rev. C **61** (2000), 064317.
42) T. Vertse, A. T. Kruppa, R. J. Liotta, W. Nazarewicz, N. Sandulescu and T. R. Werner, Phys. Rev. C **57** (1998), 3089.